Preliminary investigation of neutron shielding compounds for ARC-class tokamaks

Preliminary investigation of neutron shielding compounds for ARC-class tokamaks

Stefano Segantin[a], Samuele Meschini[a], Raffaella Testoni[a], Massimo Zucchetti[a]

[a]DENERG, Politecnico di Torino, Italy

Abstract

Radiation shielding design is a crucial step in the development of a nuclear fusion reactor. Superconducting magnets are indeed a highly engineered component whose properties are particularly sensitive to irradiation damage. In addition, novel magnet technologies, such as High Temperature Superconductors (HTS), and the attractiveness of compact tokamak designs (like Affordable Robust Compact - ARC - reactor), require an even higher precision in the shielding design. In this work most promising radiation shielding solutions for compact tokamaks are explored. The study applies a Monte Carlo particles transport technique assisted by the OpenMC code. A D-shaped model is built and ARC reactor core is considered as main case study. A detailed analysis of the radiation environment is carried out. The study then assesses the most promising compounds on the basis of most suitable cross sections, material shielding properties and space constraints. In addition, the work addresses the problem of energy deposition on the shield providing an analytical model for active cooling necessities. Results highlighted the necessity of heavy elements and high density compounds as a considerable photon flux is generated in neutron-material interactions. Tungsten borides (W_xB_y) ceramics seem to be particularly promising for shielding radiation in a compact configuration.

1. Introduction

Compactness is most certainly one of the key reasons for ARC (Affordable Robust Compact)-class tokamak attractiveness. The reactor is designed for a fusion power similar to ITER one in a tenth of ITER plasma volume. The reduced size is made possible by the high temperature superconductor magnets. HTS raise the magnetic field allowing a higher power density. Still, as the reactor size shrinks, magnets get placed closer to the plasma. The power density and the reactor compactness are cause of an increased radiation fluxes on the magnets and little room for core components. In these conditions a highly engineered radiation shield becomes necessary in order to properly shield the magnets and the surrounding components.

ARC configuration proposed by Sorbom [1] foresees a few-centimeters thick vacuum vessel placed in a liquidimmersion blanket. The blanket is a liquid lithium-fluoride and beryllium-fluoride (FLiBe) compound in its eutectic composition (2LiF-BeF_2). The thickness of the blanket can be lower than one meter in some regions of the reactor core (e.g., close to the divertor leg)[2]. A second shell-like structure with a thickness of few centimeters contains the liquid blanket. Figure 1 depicts the ARC tokamak concept configuration.

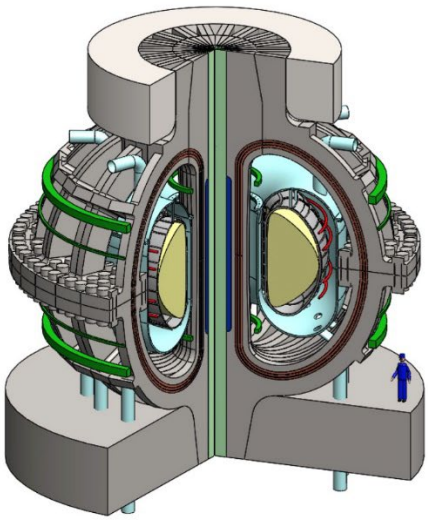

Figure 1 – Rendering of ARC reactor configuration [1].

The two shells and especially the blanket act as first neutron shield for the HTS magnets. However, Kuang [2] already highlighted the necessity of an additional neutron shield at least in some regions of the reactor core. More specifically, the poloidal field (PF) magnets that are the closest HTS to the vessel experience a prohibitive neutron flux. Nevertheless, it is likely that a shield embedding the whole blanket would be necessary anyway to reduce the radiation levels in the reactor building. Kuang [2] proposed 20 cm thick ZrH_2 specifically for reducing the neutron flux on the mentioned coils. Results including ZrH_2 suggested that the neutron shield is sufficient for the mentioned purpose. However, the reactor power density and the high neutron energy involved suggest that also gamma radiation can become harmful to sensitive functional materials such as superconductive magnets and thermal insulators. It is therefore necessary to evaluate additional backup materials for effectively shielding different forms of radiations in the limited volume available. In this framework, dense ceramics composed by a low-Z moderator element and a high-Z fast neutron absorber are here explored. Alongside ZrH_2 and the more common B_4C, tungsten-based ceramics are here proposed and analysed. This study focuses in particular on the shielding effectiveness of WC and W_xB_y compounds, which have recently gained interest in the radiation shielding field [3][4][5]. In fact, tungsten can raise the compound density while absorbing both thermal and fast neutrons. Boron, on the other hand, is a well-known absorber of thermal neutrons. Lastly, radiation energy deposition should be addressed as well. Despite the quasi-totality of the power is deposited in the blanket area, it is likely that the power deposition on the shield would be non-negligible in terms of thermal heating, ultimately requiring ad-hoc active cooling.

2. Methodology

The goal of this study is to design the radiation shields for ARC reactor taking into account both neutron and gamma radiations. The method applied is divided in four steps:

1. Identification of the most promising elements through their cross sections of relevance for the purpose. Cross sections need to be considered in the whole range of fusion neutron energy, that is, up to 14 MeV. Thermal, epithermal and fast ranges must be considered because of the blanket moderating effects. Relevant cross sections are the total cross section (n, tot), the capture cross section $(n\ ,\ \gamma\ )$ and the neutron multiplication cross section (n, Xn). Total and capture cross sections are usually considered in neutron shielding. In addition, multiplication cross section needs to be checked because of the high energy that fusion neutrons hold.
2. Selection of the compounds that feature the identified elements.

3. Neutronics modeling and simulation. The OpenMC code is applied for this purpose. The modelling strategy is fully described in the next section. Once the model is built, the shielding materials previously selected are tested. Neutronics can provide all the information needed for this work. In particular, it is possible to compute the fraction of neutrons leaking the shield and the relative energy spectra. Energy deposition is another main result of this study.
4. Analytical modelling of the radiation shield cooling system for removing the thermal power deposition.

It is worth to mention that Kuang [2] estimated the lifetime of the most endangered PF coils as a function of fast neutron fluence. This work includes Kuang's conditions (i.e., ZrH_2 neutron shield) in order to provide a direct comparison with the other compounds explored.

3. Neutronics Model

The study takes advantage of the OpenMC software and ENDF/B-VIII cross section libraries for a neutronics modeling of the ARC reactor core [6][7]. An ARC neutronics model with detailed geometry has already been designed [2]. However, the aim of this study is to build a simplified fast-running and easy-to-parametrize model. In addition, such model should be versatile in order to provide useful results adaptable also to future versions of ARC reactor and other ARC-like compact tokamaks.

This work proposes a D-shaped model with many layered cells. The whole model was divided in two regions called High Field (HF) side and Low Field (LF) side. Figure 2 displays a model section with the regions and the layers specified.

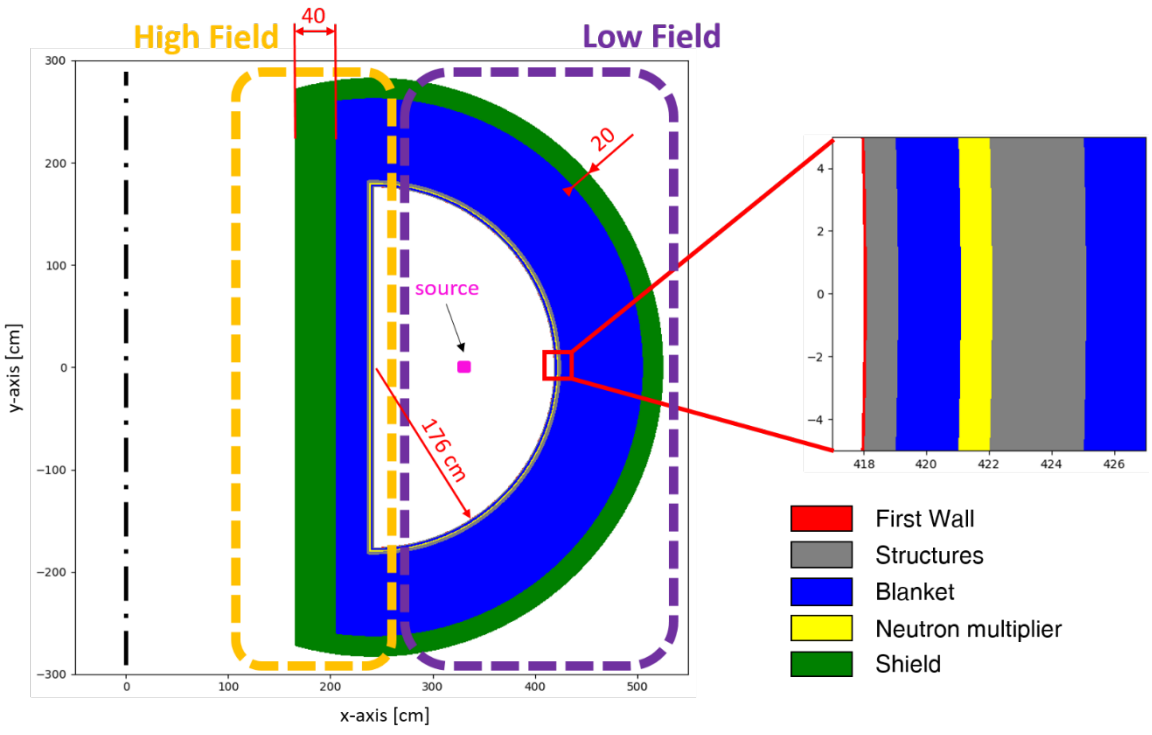

Figure 2 – Neutronics model geometry, poloidal section. All the model layers, cells and source box are displayed. Measures in cm.

The section displayed is extruded on the z-axis direction for 100 cm. ARC tokamak toroidal major radius is equal to 330 cm [1][2]. Hence, a 100 cm extrusion in the toroidal direction (i.e., along the z-axis) corresponds to a slice of about 1/21 of the whole torus. A 100 cm length for the model is considered a good trade-off between computational cost and results consistency [8]. The D-model size has been built in order to match actual ARC first wall surface, which is a key part of the strategy to provide ARC-relevant results of flux and

current [8]. For this purpose, the first wall is a perfect semi-circle of 176 cm of radius. Vacuum vessel configuration has been carefully reproduced according to Sorbom and Kuang [1][2]. Starting from the inner cell the model has 0.1 cm of first wall (FW), 1 cm of the inner structure of the vacuum vessel (STR1), 2 cm of cooling channel (channel), 1 cm of a neutron multiplier (NMULT), 3 cm of the vacuum vessel outer structure (STR2). According to Sorbom the HF side blanket has a thickness of 20 cm while the HF shield is 50 cm thick [1]. Kuang's design suggests roughly 50 cm of blanket [2]. This study proposes 30 cm of blanket and 40 cm of shield based on a minimum blanket thickness required for the effective power deposition and for breeding tritium and quantified in a previous work [9]. The LF side has much more room for components and a newer ARC version show a variable blanket thickness in the poloidal cross section [2]. This work takes the minimum thickness recorded, i.e. 80 cm, which is in correspondence of the PF coil closest to the vacuum vessel. In order to protect the mentioned coil, this model features a 20 cm thick LF shield, as proposed by Kuang [2]. All the geometry has been accurately built to be watertight. Reflective boundary conditions have been set on the two sides of the system to model toroidal continuity. Outer shield surfaces feature a vacuum boundary condition. Vacuum vessel and blanket temperatures have been set equal to 900 K while the shield temperature has been set equal to 350 K. The shield must be kept at low temperature to minimize the radiative heat transfer to the magnets.

The source has been modeled as a box of 20x20x100 cm edges (x, y and z directions, respectively). The source models the hottest region of the plasma column. 14.06 MeV neutrons are generated with an isotropic distribution and a source intensity of 9e+18 n/s. Recalling that the model is a slice of 1/21 of the whole tokamak, this intensity value corresponds to 525 MW of fusion power, according to ARC design [1][2]. Because of the high neutron absorption rates expected in the model the survival biasing variance reduction technique has been implemented [6]. The model samples 10 batches of 1e7 particles each.

The baseline configuration foresees a first wall made of tungsten (W), Inconel 718 for the two vacuum vessel structures, a beryllium neutron multiplier and a blanket of liquid FLiBe in its eutectic composition (2LiF-BeF_2) with 90% of Li-6 enrichment [1]. In addition, ZrH_2 is suggested for the neutron shield [2]. This work focuses mainly on the shielding design. Hence, vessel and blanket materials are taken accordingly to the baseline configuration. In this respect, it is worth to mention that previous studies confirmed the shielding and moderating effectiveness of 90% Li-6 enriched FLiBe [9]. Alongside the baseline ZrH_2, additional materials have been selected for the analysis. Boron carbide (B_4C) has been extensively applied as shield in thermal fission reactors. Boron has an extremely high absorption cross section for thermal neutrons. However, ARC shield is expected to experience fast neutrons mostly. In this respect, W shows a particularly high absorption cross section in the fast neutron region. W-based compounds often have high density and high total cross sections. For this reason, tungsten carbide (WC) and two types of tungsten borides (WB and WB_4) are included as case studies. Table 1 lists the material properties relevant for the neutronic modeling.

Table 1 – Composition, density, cell name in the model and reference for the materials implemented in the OpenMC model.

Material	**Composition [at. %]**	**Density** $\left[\frac{g}{cm^3}\right]$	**Model cell**	**Reference**
W	W 100	19.30	FW	[10]
Inconel 718	Ni 53 – Cr 19.06 – Fe 18.15 – Nb 5.08 – Mo 3.04 Ti 0.93 – Al 0.52 – Co 0.11 – C 0.02 – Cu 0.02 - impurities	8.19	STR1, STR2	[11]
Beryllium	Be 100	1.85	Nmult	[12]
FLiBe	F 57.14 – Li 28.57 – Be 14.29	1.96	channel, blanket	[13]

ZrH_2	Zr 33 – H 67	5.56	shield	[14]
B_4C	B 80 – C 20	2.51	shield	[15]
WC	W 50 – C 50	15.32	shield	[3]
WB	W 50 – B 50	12.91	shield	[3]
WB_4	W 20 – B 80	8.23	shield	[3]

Six different compounds are analyzed.

- FLiBe: the shielding region is covered by FLiBe in an expanded blanket – no shield scenario
- ZrH_2: the baseline shielding material
- B_4C: widely adopted in thermal fission.
- WC, WB, WB_4: advanced materials for compact shielding.

Figure 3 depicts the macroscopic cross sections of the six compounds analyzed. Heavy metal-based compounds show higher neutron interaction probability than lighter compounds in the fast neutron region. FLiBe and, especially, boron carbide show a high cross section in the epithermal and thermal region. Tungsten borides show high neutron interaction probabilities both in thermal and fast regions. This suggests a likely superior shielding capability in fusion reactor environments. Nevertheless, for very fast neutrons, including the 14 MeV fusion neutrons, Zr and W have neutron absorption and neutron multiplication cross sections both relatively high. Hence, neutronics modeling and simulation on specific reactor configurations are necessary to assess the actual shielding capabilities of Zr- and W-based compounds.

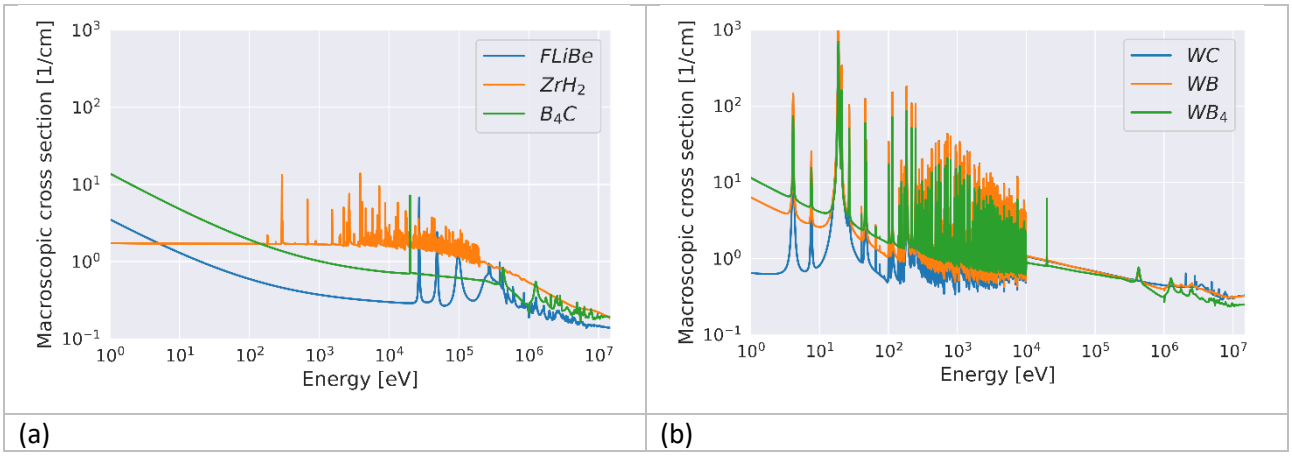

Figure 3 – Macroscopic neutron cross sections for the 6 shielding compounds analysed. (a) displays the results for FLiBe, ZrH_2 and B_4C shields, (b) displays WC, WB and WB_4 shield results. Data from ENDF/B-VIII library [7].

Flux and power deposition on the shielding cells, currents entering and exiting the shield surfaces have been tallied for both neutrons and photons. Lastly, a sensitivity analysis on B-10 enrichment fraction for boron-based shields has been carried out. In fact, natural isotopic composition of the key absorbing element boron 80.01% B-11 and 19.9% B-10 with the latter holding a neutron capture cross section that is orders of magnitude higher than the former [7].

Each simulation required about 4 hours on an AMD Ryzen 5000 series CPU with 8 dedicated threads. Additional runs were performed for a better convergence of the energy spectra with 10e8 particles per batch with 10 batches.

4. Results

Alongside shielding-relevant results the tritium breeding ratio (TBR) of the model has been checked to ensure the reactor performance. In all the configurations the TBR was found to be between 1.055 and 1.065. The type of shield behind the blanket is not supposed to play a major role in tritium breeding. However, a slight difference is here observed, as shown in Figure 4. Zr and W behave as good fast neutron reflectors, especially

if coupled with a low absorbing element, like in the case of zirconium hydride and tungsten carbide. The reflecting effect of the shielding compounds on the TBR is recorded mainly in the HF region, where the blanket is only 30 cm thick.

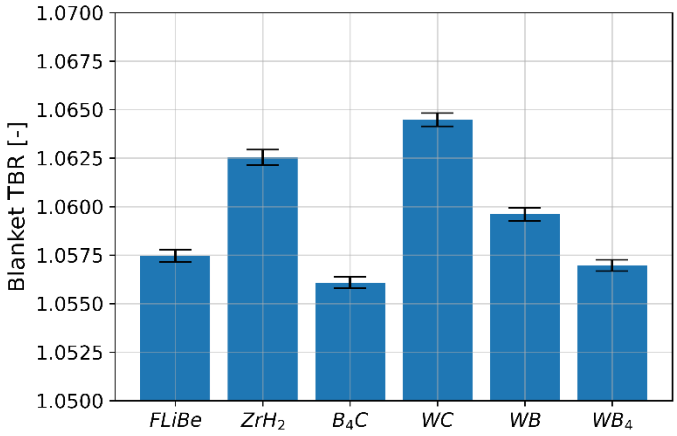

Figure 4 – Blanket tritium breeding ratio for different shielding materials. Error bars account for three times the standard deviation provided by OpenMC.

Table 2 summarizes the results of neutron and photon current exiting the shield the shields from the HF and LF sides.

Table 2 – Neutron and photon currents exiting the shield from the high and low field sides.

	Neutron Current $\frac{n}{s \cdot cm^2}$		**Photon Current $\frac{p}{s \cdot cm^2}$**	
	High Field	**Low Field**	**High Field**	**Low Field**
FLiBe	1.35e11±2.07e8	1.19e10±7.86e7	6.23e11±8.93e8	1.11e11±2.01e8
ZrH2	1.94e10±7.93e8	3.71e9±5.56e7	2.42e10±1.37e8	1.03e10±9.05e7
B4C	2.67e10±1.50e8	4.64e9±4.40e7	3.87e11±7.00e8	9.26e10±2.93e8
WC	1.80e10±1.17e8	6.41e9±6.25e7	2.61e9±4.33e7	7.34e8±1.55e7
WB	6.32e9±8.20e7	3.47e9±3.48e7	5.71e8±2.99e7	3.06e8±1.52e7
WB4	1.12e10±8.75e7	3.69e9±5.11e7	1.92e9±3.86e7	1.11e9±3.35e7

Fluxes exiting the shield reach the same order of magnitude with all the shielding materials, exception made for the FLiBe case study. Figure 5 displays the inverse of the shielding effectiveness of the materials considered, computed as $\frac{J_o}{J_i}$ where J_i is the current entering the shield and J_o is the current exiting the shield. The shield out-in current ratio $\left(\frac{J_o}{J_i}\right)$ has been computed for both neutron and photon particles in the HF side.

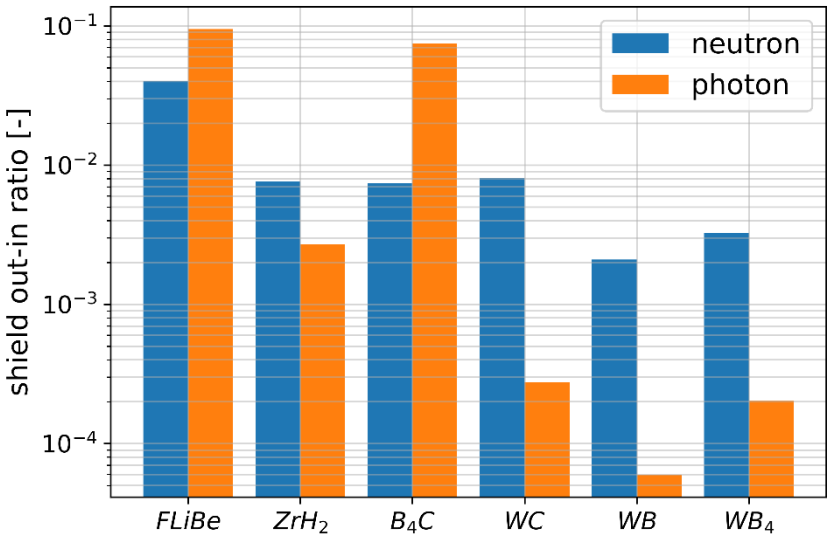

Figure 5 – Inverse of shielding effectiveness (shield out-in current ratio) of the HF shield of the model. Computed for neutrons and photons.

All shielding materials perform better than FLiBe in shielding both neutrons and photons. Boron carbide is not particularly effective in shielding photons. This is mainly due to the low Z elements and low density compound. Tungsten borides show the best performances, reducing by two orders of magnitude the fluxes of both the particle species considered. Figure 6 shows how B-10 enrichment fraction affects the shielding effectiveness on HF side shields. The figure shows the neutron current exiting the shield from the high field side.

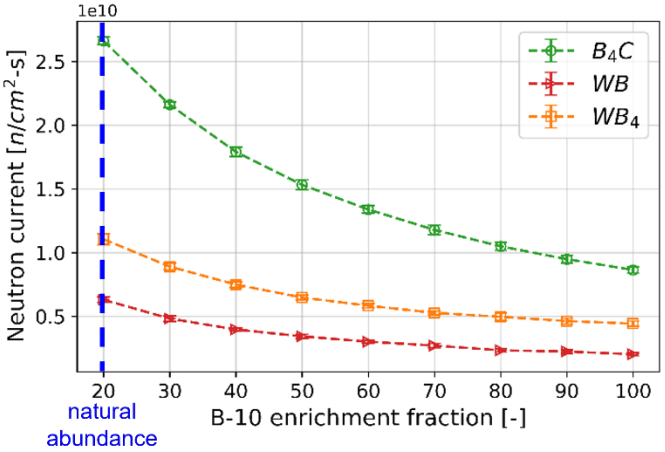

Figure 6 – Neutron current exiting the HF shield as a function of the shield B-10 enrichment fraction. Sensitivity analysis carried out on boron-based shielding materials. Error bars account for three times the standard deviation provided by OpenMC.

A boron-based shield with an ideal B-10 100% enrichment fraction is able to halve the neutron current exiting the shield in all the cases studied.

Figure 7 displays the energy spectra of neutron currents exiting the HF shield, assuming a natural isotopic composition of boron.

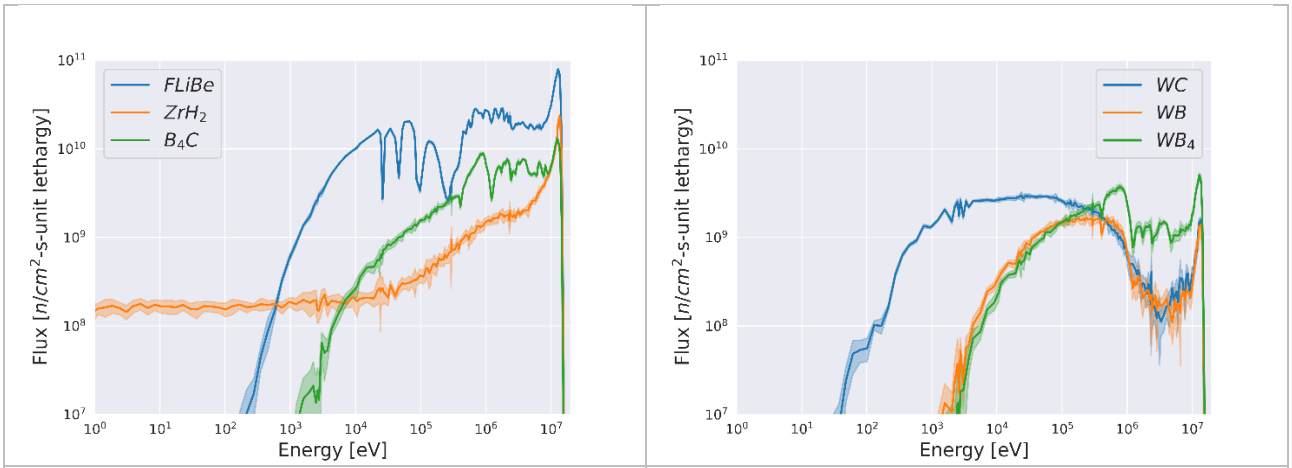

Figure 7 – Energy spectra of the neutron current exiting the shield form the high field side. (a) displays the results for FLiBe, ZrH_2 and B_4C shields, (b) displays WC, WB and WB_4 shield results. Coloured areas account for three standard deviations. Results are per unit lethargy.

Neutrons exiting the whole blanket & shield system are still very energetic. Although the peak at 14.06 MeV has been effectively moderated, almost all the spectra stand mainly in the fast region. One exception is made by ZrH_2 shield. Because of the high hydrogen content, zirconium dihydride successfully moderated most of the neutrons down to the thermal-epithermal side of the spectrum. Considering the differences in the spectra, it is worth to provide the fraction of fast neutrons (energy > 0.1 MeV) that exit the shield for each compound. It is indeed known that fast neutrons are of much more concern with respect thermal and epithermal neutrons [16][17][18]. Once again, results shown focus on the HF side of the reactor. Table 3 lists the current of fast neutrons exiting the HF side shield and their fraction with respect the total current, for each shielding compound.

Table 3 – Fast neutron current exiting the HF shield and fraction of fast neutrons over the total current as a percentage.

	Fast neutron Current $\frac{n}{s \cdot cm^2}$	**Fast-to-total fraction %**
FLiBe	9.58e10±2.86e9	71
ZrH2	1.20e10±1.11e9	62
B4C	2.48e10±1.41e9	93
WC	5.19e9±6.55e8	29
WB	4.17e9±5.69e8	66
WB4	9.56e9±9.49e8	86

From the second column it may seem that WC is a better moderator than other compounds. Nonetheless, comparing it with the first column, it is possible to notice that also boron-based compounds are good moderators, but boron has also a much higher thermal and epithermal neutron absorption capability than the other elements here considered. Namely, the main difference between WC and W_xB_y is that carbon moderates effectively but does not absorb, while boron moderates and absorbs effectively. Boron-based compounds then tend to cut off relatively quickly low-energy neutrons from the population, letting through only the fast component of the neutron flux. Focusing on fast neutrons, tungsten-based compounds confirm their superior performance as shields.

Lastly, Figure 8 shows the power deposition in each shield type.

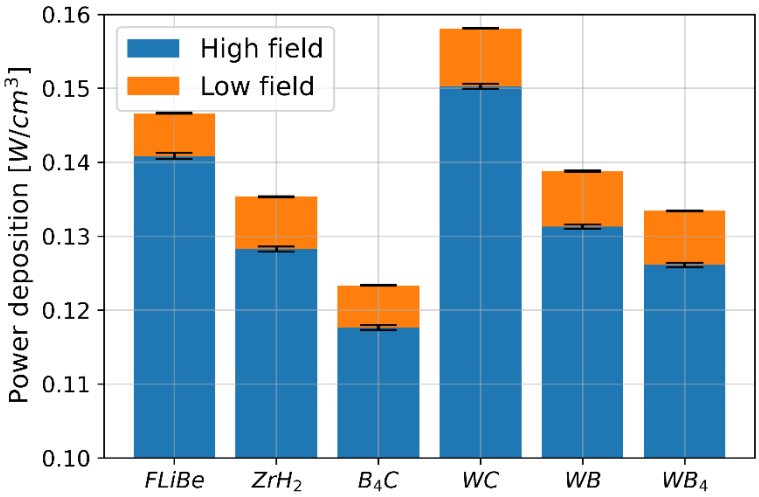

Figure 8 – Power deposition on the neutron shield for different shielding compounds. Error bars account for three times the standard deviation provided by OpenMC.

The high field side of the shield is expected to experience a larger fraction of power deposition with respect the low field side because of the proximity to the vacuum vessel and the higher thickness. All the shield designs get a power deposition of 5-7 MW_{th}. Such power is about 1% of the whole reactor thermal power but it is high enough to require an active cooling system.

4.1 Cooling system thermal design

A preliminary design of the shield cooling system has been carried out based on the results from the neutronics analysis. The power density was measured by *heating* tallies placed in the HF and LF cells. The design is proposed for the WC shield, HF side, which presents the highest power deposition (Figure 8). The power density is $0.146\ W/cm^3$ in the HF shield and $9 \cdot 10^{-3}\ W/cm^3$ in the LF shield. A 10% safety factor has been considered for the power removal capability of the cooling system. The volume of the HF shielding cell is $2.34\ m^3$ (OpenMC returns the cell volume as output), leading to a thermal power of $\sim 370\ kW$ to be removed. The shield operating temperature has been assumed equal to 350 K to limit radiative heat transfer towards the surrounding structure, especially the superconducting magnet jackets. Such a low operating temperature cuts off FLiBe as possible coolant.

Water is not suitable as coolant as well because of its strong chemical reactivity with Li. The exothermal reaction between water and Lithium produces free hydrogen, which can generate fires and explosions. Additionally, the production of a gas in a confined volume leads to a pressurization that may end in a confinement failure [19]. The proximity of the shielding cooling circuit to the FLiBe tank (i.e., to a large Li mass) precludes water as a candidate coolant.

An inert gas is a natural choice to prevent chemical reactions between circulating fluids. Furthermore, a gas can easily operate at a temperature suitable for the shield. Therefore, helium is chosen as coolant. The inlet coolant temperature is set at 275 K, and the coolant pressure is set at 10 bar. Each coolant channel is 586 cm long (i.e., equal to the shield height) and has a 1 cm diameter (D_{ch}). Channels are located at the shield centerline ($R_{shield} = 185\ cm$) and are equally spaced. The pitch (p_{ch}) is 10 cm. This configuration results in 117 channels ($n_{channels} = \frac{2\pi R_{shield}}{p_{ch}+D_{ch}}$) to cool the entire HF side shield. Size and pitch of the cooling channels have been designed in order to affect as little as possible the shielding effectiveness of the component still ensuring a sufficient cooling capability. Indeed, in this suggested design the channels volume account for less than 1% of the total volume of the shield. Nonetheless, once the detailed design of an ARC-class machine will

be performed, the effect of the coolant pipes and specific geometry choices on the overall shielding effectiveness should be assessed in dedicated simulations.

The coolant wall temperature has been assumed constant, $T_{wall} = 350\ K$. Under this assumption, the outlet coolant temperature can be found as:

$$T_{out} = T_{wall} + (T_{in} - T_{wall}) \exp\left(-\frac{A_{tot}\bar{h}}{\dot{m}c_p}\right)$$

Where T_{in} [K] is the inlet coolant temperature, A [m^2] is total heat exchange area, $\bar{h}$ [W/(m^2 K)] is the average heat transfer coefficient along the channel, $\dot{m}$ [kg/s] is the coolant mass flow rate and c_p [J/(Kg K)] is the specific heat capacity at constant pressure. The average heat transfer coefficient was computed from the Dittus-Boelter correlation, which is fully applicable in the case under study $\left(Re > 10^4, 0.6 < Pr < 160, \frac{L}{D} > 10\right)$ [20]. The results of the analysis are shown in Table 4.

Table 4 - Results from the thermal-hydraulics analysis of a shield channel.

Quantity	Symbol	Value
Number of channels	$\boldsymbol{n_{channels}}$	**117**
Reynolds number	Re	$1.04 \cdot 10^4$
Prandtl number	Pr	0.6616
Nusselt number	Nu	33.6
Average heat transfer coefficient $\left(\frac{W}{m^2 \cdot K}\right)$	$\bar{h}$	526
Coolant outlet temperature (K)	T_{out}	339
Coolant mass flow rate (channel) $\left(\frac{kg}{s}\right)$	$\dot{m}$	$9.4 \cdot 10^{-3}$
Coolant mass flow rate (total) $\left(\frac{kg}{s}\right)$	$\dot{m}_{tot}$	1.10
Coolant velocity $\left(\frac{m}{s}\right)$	v_{He}	13

Helium flow in the shield channels is slightly turbulent ($Re \sim 10^4$), and the required cooling can be achieved with an acceptable gas velocity. The frictional pressure drop in a channel has been computed from Moody's diagram assuming smooths pipes [21]. The pressure drop in each channel is $\Delta p = f \frac{L_{ch}}{D_{ch}} \frac{\bar{\rho}_{He} v_{He}^2}{2} = 2630\ Pa$, where L_{ch} is the channel length, and $\bar{\rho}_{He}$ is the average helium density. Despite the entire cooling circuit has not been designed yet, a pressure drop of 2.6 kPa along the channel (for a coolant pressure of 10 bar) is a very promising result.

5. Discussion

From a neutronics viewpoint, effectiveness of providing a tritium self-sufficiency is the first thing to assess regarding a tokamak core configuration. TBR values found are not considered sufficient for operating the reactor in real conditions [22]. Especially considering that this simplified model does not take into account in-vessel component, divertors and additional vessel-tank structures. Still, previous studies provide effective solutions to raise the TBR above the minimum thresholds [8][9]. ARC configuration is thus not expected to raise concerns regarding low TBR.

Shielding materials have shown slightly different behaviors. Boron carbide effectiveness is not optimal for fusion spectra especially because of photon transport. From results it is clear that denser shields based on heavy metals would help solving the photon issue. Proposed W-based ceramics hold better performances than the baseline ZrH_2. WB_4, for instance, stops three times more particles than ZrH_2 with equal thickness. Consistently with Kuang's evaluations for ZrH_2 [2], WB_4 would allow a lifetime of the most endangered

magnet of almost four decades. Nonetheless, ZrH_2 seems to be a better moderator. This is true only for neutrons in the range 1 keV – 2 MeV, which are effectively moderated to thermal energies. Zirconium dihydride shows still a peak of neutrons at 14 MeV that is not observed in the other metal-based shields. Tungsten borides hold the best performances in terms of neutron and photon shielding capability and a relatively good effectiveness in mitigating the 14 MeV neutron peak. In addition, a boron-based shield holds the additional possibility of further improving the shielding effectiveness by a B-10 enrichment technique. Raising the B-10 isotopic concentration from natural (i.e. about 20%) to 90-100% would allow to double the shielding effectiveness. However, considering the performance of metal-based compounds are of similar magnitudes, it is likely that in commercial reactors the choice will be economics-driven.

LF side shows flux values similar to the HF side, but it has some room for optimization. It is possible to reduce the blanket thickness by several tens of cm in favor of additional shield where needed without undermine TBR nor the effective thermal power [9]. The HF side seems to be more concerning. It is not possible to further reduce the blanket thickness for TBR and effective power deposition. It may also be the culprit for the exclusion of other blanket compounds with poor shielding capabilities as well as lower Li-6 enrichment fractions for FLiBe, as discussed in previous works [9]. It is likely that the HF side would require a high-performance – compact shield (i.e. tungsten borides) while LF could absorb the cost with cheaper shielding compounds.

There is however a downside to the use of heavy metal-based shields. The high density of such compounds may require for additional structural analysis and feasibility considerations. In a preliminary assumption of a shield designed as it is proposed in this model and embedding the whole reactor, the volumes of high field and low field shields would be as high as 26 and 50 m^3 respectively. The low field monolith would have a mass of about 125 tons of B_4C or 770, 650 or 410 tons of WC, WB and WB_4, respectively. The low field shield alone would most likely overcome by hundreds of tons the total weight foreseen for such component in its totality for ARC (i.e. about 380 tons [1]), if made of some tungsten compound. Clearly, on the low field side, the weight can be dramatically reduced by wrapping just the magnets with the heavy compound and using lighter compounds in non-magnets regions, in a sort of sliced shield. Nevertheless, the same operation does not seem to be feasible for the high field shield, considering that it has to protect the whole central solenoid. On the high field side, a monolithic shield embedding the central solenoid would have a mass of roughly 65, 400, 330 or 210 tons of B_4C, WC, WB or WB_4, respectively. If neutrons and photon transport highlighted the superior performances of tungsten-based compounds, the necessity for a lightweight shield identifies tungsten borides as the best tradeoff option.

Kuang et al. [2] suggest placing the shield inside the breeding blanket mainly to allow an easy assembly and disassembly of the reactor core. In addition, such configuration would allow the FLiBe in the tank to work as a coolant for the shield. However, it is likely that ceramic materials such as the shield here investigated would easily deteriorate at 900-1000 K in a flowing molten salt environment. Hence, it is here suggested to position the neutron shields outside the blanket tank in order to mitigate corrosion and thermally-induced deterioration. An actively cooled shield at 300-400 K would also work as additional thermal shield between the 900 K tank and the 20 K magnets. In this instance, the required power removal can be achieved by a 1.1 kg/s He flow at 10 bar and an inlet temperature of 275 K. This value should be easily obtainable by exploiting the low temperature sink of the cryogenic circuit. If a suitable connection with the cryogenic system cannot be found, the inlet coolant temperature may be increased up to 293 K (i.e., room temperature) with no particular issues. It should be noted that the outlet coolant temperature is compatible with the sweep gas temperature required in a double wall heat exchanger or in the power cycle in the case of a He-based Brayton [23][24]. A single He circuit may be considered to fulfil both the functions if the pressure between the two systems (shield cooling and heat exchanger) matches. This can be done by setting the shield coolant pressure at 10 bar, as done in this work.

6. Conclusion

This work focused on the exploration of the shielding effectiveness of metal-based ceramics and the design of neutron shields for ARC reactor and compact tokamaks. A D-shaped neutronics model that mimics ARC core configuration has been built. Such model provides results consistent with models having a more detailed geometry but it runs faster and its results are much more versatile for future ARC versions and other compact tokamaks. Firstly, a slightly poor tritium breeding capability related to the Inconel-based vacuum vessel has been observed and more transparent structural materials should be adopted. Secondly, the high field side of the tokamak has proven to suffer the compact nature of the machine. HF side is likely to fix the design to a 30 cm thick, 90% Li-6 enriched FLiBe blanket and 40 cm thick tungsten boride shield, for the TBR-shielding trade-off. Each of those elements maximize the shielding without undermine the TBR nor the effective power deposition in the blanket. Tungsten-based compounds showed indeed better performances than the baseline zirconium dihydride. In addition, boron-based compounds have the possibility of further doubling the shielding effectiveness with no-additional thickness by a B-10 enrichment technique. Nonetheless, they raise concerns regarding the total weight of the shielding components. If a heavy metal-based compound is required for shielding a structural analysis should be considered as well as a weight optimization oriented design of the component. In this instance WB_4 seems to have the best shielding-weight tradeoff results. Because of the thick nature of the shields, the power deposition on such components resulted big enough to require active cooling. A He-based cooling system is suitable to the purpose without particularly increasing the machine complexity. Helium can in fact be shared with the heat exchanger system and/or the power cycle.

In future works, the model will be built with an increased level of detail. A toroidal geometry will be modelled as well as the main toroidal and poloidal field coils. Alongside the fluence on the magnets, future works will evaluate the dose on surroundings area providing additional shielding components if required. Studies will then assess the radioactive inventories of irradiated shields. Lastly, the thermal design of the shielding cooling system will be assisted by finite elements method tools.

References

[1] Sorbom, B. N., et al. "ARC: A compact, high-field, fusion nuclear science facility and demonstration power plant with demountable magnets." Fusion Engineering and Design 100 (2015): 378-405.

[2] Kuang, A. Q., et al. "Conceptual design study for heat exhaust management in the ARC fusion pilot plant." Fusion Engineering and Design 137 (2018): 221-242.

[3] Windsor, C. G., et al. "Design of cemented tungsten carbide and boride-containing shields for a fusion power plant." Nuclear Fusion 58.7 (2018): 076014.

[4] Athanasakis, M., et al. "A high temperature W_2B cermet for compact neutron shielding." arXiv preprint arXiv:1912.04671 (2019).

[5] Giménez, M. A. N., et al. "Tungsten carbide compact primary shielding for small medium reactor." Annals of Nuclear Energy 116 (2018): 210-223.

[6] Romano, P. K., et al. "OpenMC: A state-of-the-art Monte Carlo code for research and development." Annals of Nuclear Energy 82 (2015): 90-97.

[7] Brown, D. A., et al. "ENDF/B-VIII. 0: the 8th major release of the nuclear reaction data library with CIELO-project cross sections, new standards and thermal scattering data." Nuclear Data Sheets 148 (2018): 1-142.

[8] Segantin, S., et al. "Optimization of tritium breeding ratio in ARC reactor." Fusion Engineering and Design 154 (2020): 111531.

[9] Segantin, S., et al. "Neutronic comparison of liquid breeders for ARC-like reactor blankets." Fusion Engineering and Design 160 (2020): 112013.

[10] Davey, W. P. "The lattice parameter and density of pure tungsten." Physical Review 26.6 (1925): 736.

[11]Thomas, A., et al. "High temperature deformation of Inconel 718." Journal of materials processing technology 177.1-3 (2006): 469-472.
[12]Materion website “Physics and chemistry of beryllium”. https://materion.com/-/media/files/beryllium/beryllium-materials/mb-003physicsandchemistryofberyllium.pdf (last view: November 2021).
[13]Nagasaka, T., et al. “Progress in flibe corrosion study toward material research loop and advanced liquid breeder blanket”. No. NIFS--925. National Inst. for Fusion Science, 2008.
[14]Americanelements website “Zirconium Hydride”. https://www.americanelements.com/zirconium-hydride-7704-99-6 (last view: November 2021).
[15]Bouchacourt, M., et al. "The properties and structure of the boron carbide phase." Journal of the Less Common Metals 82 (1981): 227-235.
[16]Bromberg, L., et al. "Options for the use of high temperature superconductor in tokamak fusion reactor designs." Fusion Engineering and Design 54.2 (2001): 167-180.
[17]Fischer, David X., et al. "The effect of fast neutron irradiation on the superconducting properties of REBCO coated conductors with and without artificial pinning centers." Superconductor Science and Technology 31.4 (2018): 044006.
[18]Zhai, Y., et al. "Conceptual design of HTS magnets for fusion nuclear science facility." Fusion Engineering and Design 168 (2021): 112611.
[19]Utschig, T. T., et al. "Lithium safety in fusion systems (ITER)." *Fusion engineering and design* 51 (2000): 641-645.
[20]Bergman, T., et al., Fundamentals of heat and mass transfer, 7th ed. ,Hoboken: John Wiley & Sons, 2011.
[21]Moody, L. F. "Friction factors for pipe flow." Trans. Asme 66 (1944): 671-684.
[22]Abdou, M., et al., “Physics and technology considerations for the deuterium-tritium fuel cycle and conditions for tritium fuel self-sufficiency” Nucl. Fusion, 61, 1, (2021),doi: 10.1088/1741-4326/abbf35.
[23]Meschini, S., et al. “Engineering design status and preliminary safety analysis of ARC pilot plant” submitted to Fusion Engineering and Design in November 2021.
[24]Segantin, S., et al. "Exploration of power conversion thermodynamic cycles for ARC fusion reactor." Fusion Engineering and Design 155 (2020): 111645.